NOAA Technical Memorandum NWS ER-75

WIND SHEAR AS A PREDICTOR OF SEVERE WEATHER FOR THE EASTERN UNITED STATES

Hugh M. Stone
National Weather Service Eastern Region
Garden City, New York

Scientific Services Division
Eastern Region Headquarters
January 1988

U.S. DEPARTMENT OF COMMERCE / National Oceanic and Atmospheric Administration / National Weather Service

NOAA TECHNICAL MEMORANDA
National Weather Service, Eastern Region Subseries

The National Weather Service Eastern Region (ER) Subseries provides an informal medium for the documentation and quick dissemination of results not appropriate, or not yet ready for formal publications. The series is used to report on work in progress, to describe technical procedures and practices, or to relate progress to a limited audience. These Technical Memoranda will report on investigations devoted primarily to regional and local problems of interest mainly to ER personnel, and hence will not be widely distributed.

Papers 1 to 22 are in the former series, ESSA Technical Memoranda, Eastern Region Technical Memoranda (ERTM); papers 23 to 37 are in the former series, ESSA Technical Memoranda, Weather Bureau Technical Memoranda (WBTM). Beginning with 38, the papers are now part of the series, NOAA Technical Memoranda NWS.

Papers 1 to 22 are available from the National Weather Service Eastern Region, Scientific Services Division, 585 Stewart Avenue, Garden City, N.Y. 11530. Beginning with 23, the papers are available from the National Technical Information Service, U.S. Department of Commerce, Sills Bldg., 5285 Port Royal Road, Springfield, Va. 22151. Prices vary for paper copy; $2.25 microfiche. Order by accession number shown in parentheses at end of each entry.

ESSA Technical Memoranda

ERTM 1 Local Uses of Vorticity Prognoses in Weather Prediction. Carlos R. Dunn April 1965
ERTM 2 Application of the Barotropic Vorticity Prognostic Field to the Surface Forecast Problem. Silvio G. Simplicio. July 1965
ERTM 3 A Technique for Deriving an Objective Precipitation Forecast Scheme for Columbus, Ohio. Robert Kuessner. September 1965
ERTM 4 Stepwise Procedures for Developing Objective Aids for Forecasting the Probability of Precipitation. Carlos R. Dunn. November 1965
ERTM 5 A Comparative Verification of 300 mb. Winds and Temperatures Based on NMC Computer Products Before and After Manual Processing. Silvio G. Simplicio. March 1966
ERTM 6 Evaluation of OFDEV Technical Note No. 17. Richard M. DeAngelis. March 1966
ERTM 7 Verification of Probability of Forecasts at Hartford, Connecticut, for the Period 1963-1965. Robert B. Wassall. March 1966
ERTM 8 Forest-Fire Pollution Episode in West Virginia November 8-12, 1964. Robert O. Woodfall. April 1966
ERTM 9 The Utilization of Radar in Meso-Scale Synoptic Analysis and Forecasting. Jerry D. Hill. March 1966
ERTM 10 Preliminary Evaluation of Probability of Precipitation Experiment. Carlos R. Dunn. May 1966
ERTM 11 Final Report. A Comparative Verification of 300 mb. Winds and Temperatures Based on NMC Computer Products Before and After Manual Processing. Silvio G. Simplicio. May 1966
ERTM 12 Summary of Scientific Services Division Development Work in Sub-Synoptic Scale Analysis and Prediction - Fiscal Year 1966. Fred L. Zuckerberg.
ERTM 13 A Survey of the Role of Non-Adiabatic Heating and Cooling in Relation of the Development of Mid-Latitude Synoptic Systems. Constantine Zois. July 1966
ERTM 14 The Forecasting of Extratropical Onshore Gales at the Virginia Capes. Glen V. Sachse. August 1966
ERTM 15 Solar Radiation and Clover Temperatures. Alex J. Kish. September 1966
ERTM 16 The Effects of Dams, Reservoirs and Levees on River Forecasting. Richard M. Greening. September 1966
ERTM 17 Use of Reflectivity Measurements and Reflectivity Profiles for Determining Severe Storms. Robert E. Hamilton. October 1966
ERTM 18 Procedure for Developing a Nomograph for Use in Forecasting Phenological Events from Growing Degree Days. John C. Purvis and Milton Brown. December 1966
ERTM 19 Snowfall Statistics for Williamsport, Pa. Jack Hummel. January 1967
ERTM 20 Forecasting Maturity Date of Snap Beans in South Carolina. Alex J. Kish. March 1967
ERTM 21 New England Coastal Fog. Richard Fay. April 1967
ERTM 22 Rainfall Probability at Five Stations Near Pickens, South Carolina, 1957-1963. John C. Purvis. April 1967
WBTM ER 23 A Study of the Effect of Sea Surface Temperature on the Areal Distribution of Radar Detected Precipitation Over the South Carolina Coastal Waters. Edward Paquet. June 1967 (PB-180-612)
WBTM ER 24 An Example of Radar as a Tool in Forecasting Tidal Flooding. Edward P. Johnson. August 1967 (PB-180-613)
WBTM ER 25 Average Mixing Depths and Transport Wind Speeds over Eastern United States in 1965. Marvin E. Miller. August 1967 (PB-180-614)
WBTM ER 26 The Sleet Bright Band. Donald Marier. October 1967 (PB-180-615)
WBTM ER 27 A Study of Areas of Maximum Echo Tops in the Washington, D.C. Area During the Spring and Fall Months. Marie D. Fellechner. April 1968 (PB-179-339)
WBTM ER 28 Washington Metropolitan Area Precipitation and Temperature Patterns. C.A. Woollum and N.L. Canfield. June 1968 (PB-179-340)
WBTM ER 29 Climatological Regime of Rainfall Associated with Hurricanes after Landfall. Robert W. Schoner. June 1968 (PB-179-341)
WBTM ER 30 Monthly Precipitation - Amount Probabilities for Selected Stations in Virginia. M.H. Bailey. June 1968 (PB-179-342)
WBTM ER 31 A Study of the Areal Distribution of Radar Detected Precipitation at Charleston, S.C. S.K. Parrish and M.A. Lopez. October 1968 (PB-180-480)
WBTM ER 32 The Meteorological and Hydrological Aspects of the May 1968 New Jersey Floods. Albert S. Kachic and William Long. February 1969 (Revised July 1970) (PB-194-222)
WBTM ER 33 A Climatology of Weather that Affects Prescribed Burning Operations at Columbia, South Carolina. S.E. Wasserman and J.D. Kanupp. December 1968 (COM-71-00194)
WBTM ER 34 A Review of Use of Radar in Detection of Tornadoes and Hail. R.E. Hamilton. December 1969 (PB-188-315)
WBTM ER 35 Objective Forecasts of Precipitation Using PE Model Output. Stanley E. Wasserman. July 1970 (PB-193-378)
WBTM ER 36 Summary of Radar Echoes in 1967 Near Buffalo, N.Y. Richard K. Sheffield. September 1970 (COM-71-00310)
WBTM ER 37 Objective Mesoscale Temperature Forecasts. Joseph P. Sobel. September 1970 (COM-71-0074)

NOAA Technical Memoranda NWS

NWS ER 38 Use of Primitive Equation Model Output to Forecast Winter Precipitation in the Northeast Coastal Sections of the United States. Stanley E. Wasserman and Harvey Rosenblum. December 1970 (COM-71-00138)
NWS ER 39 A Preliminary Climatology of Air Quality in Ohio. Marvin E. Miller. January 1971 (COM-71-00204)
NWS ER 40 Use of Detailed Radar Intensity Data in Mesoscale Surface Analysis. Robert E. Hamilton. March 1971 (COM-71-00573)
NWS ER 41 A Relationship Between Snow Accumulation and Snow Intensity as Determined from Visibility. Stanley E. Wasserman and Daniel J. Monte May 1971 (COM-71-00763)
NWS ER 42 A Case Study of Radar Determined Rainfall as Compared to Rain Gage Measurements. Martin Ross. July 1971 (COM-71-00897)
NWS ER 43 Snow Squalls in the Lee of Lake Erie and Lake Ontario. Jerry D. Hill. August 1971 (COM-72-00959)
NWS ER 44 Forecasting Precipitation Type at Greer, South Carolina. John C. Purvis. December 1971 (COM-72-10332)
NWS ER 45 Forecasting Type of Precipitation. Stanley E. Wasserman. January 1972 (COM-72-10316)
NWS ER 46 An Objective Method of Forecasting Summertime Thunderstorms. John F. Townsend and Russell J. Younkin. May 1972 (COM-72-10765)
NWS ER 47 An Objective Method of Preparing Cloud Cover Forecasts. James R. Sims. August 1972 (COM-72-11382)
NWS ER 48 Accuracy of Automated Temperature Forecasts for Philadelphia as Related to Sky Condition and Wind Direction. Robert B. Wassall. September 1972 (COM-72-11473)
NWS ER 49 A Procedure for Improving National Meteorologiacal Center Objective Precipitation Forecasts. Joseph A. Ronco, Jr. November 1972 (COM-73-10132)
NWS ER 50 PEATMOS Probability of Precipitation Forecasts as an Aid in Predicting Precipitation Amounts. Stanley E. Wasserman. December 1972 (COM-73-10243)
NWS ER 51 Frequency and Intensity of Freezing Rain/Drizzle in Ohio. Marvin E. Miller. February 1973 (COM-73-10570)
NWS ER 52 Forecast and Warning Utilization of Radar Remote Facsimile Data. Robert E. Hamilton. July 1973 (COM-73-11275)
NWS ER 53 Summary of 1969 and 1970 Public Severe Thunderstorm and Tornado Watches Within the National Weather Service, Eastern Region. Marvin E. Miller and Lewis H. Ramey. October 1973 (COM-74-10160)
NWS ER 54 A Procedure for Improving National Meteorological Center Objective Precipitation Forecasts - Winter Season. Joseph A. Ronco, Jr. November 1973 (COM-74-10200)
NWS ER 55 Cause and Prediction of Beach Erosion. Stanley E. Wasserman and David B. Gilhousen. December 1973 (COM-74-10036)
NWS ER 56 Biometeorological Factors Affecting the Development and Spread of Plant Diseases. V. J. Valli. July 1974 (COM-74-11625/AS)
NWS ER 57 Heavy Fall and Winter Rain In The Carolina Mountains. David B. Gilhousen. October 1974 (COM-74-11761/AS)
NWS ER 58 An Analysis of Forecasters' Propensities In Maximum/Minimum Temperature Forecasts. I. Randy Racer. November 1974 (COM-75-10063/AS)

(Continued On Inside Rear Cover)

NOAA TECHNICAL MEMORANDUM NWS ER-75

WIND SHEAR AS A PREDICTOR OF SEVERE WEATHER FOR THE EASTERN UNITED STATES

Hugh M. Stone
National Weather Service Eastern Region
Garden City, New York

Scientific Services Division
Eastern Region Headquarters
January 1988

WIND SHEAR AS A PREDICTOR OF SEVERE WEATHER FOR THE EASTERN UNITED STATES

Hugh M. Stone

Eastern Region Headquarters
National Weather Service, NOAA
Garden City, New York

1. INTRODUCTION

Various numerical and observational studies have indicated that wind shear may be useful in explaining and possibly forecasting the type of convective storms that develop under unstable atmospheric conditions. Most of the observational data supporting the results of the numerical experiments are taken from the Great Plains region of the United States, an area well known for strong thunderstorm activity. In this study we seek to identify relationships between various measures of wind shear and stability and the occurrence of severe weather in the eastern United States. We will show that some good relationships do exist, that may be useful in assessing afternoon severe weather potential.

Convective storms evolve into many complex forms, but they may be loosely classified into three types: single cell, multicell, and supercell. The single cell is the most basic unit of convection consisting of a single updraft, usually occurring in light wind shear conditions, with the cool air from the downdraft spreading equally in all directions. This cuts off the supply of warm moist air to the cell and its lifetime is short.

Multicell convection starts with a single cell growing in a moderate wind shear environment, which causes enhanced convergence on a portion of the outflow boundary, usually in the direction of storm movement, so new cells continually develop on the boundary. The motion of the storm may differ from the motion of individual cells due to the propagation of new cells. The two motions are identical only when new cells develop directly in the path of the older cells. Severe weather, usually high winds and hail may be associated with multicell storms along with some tornadoes that are usually short lived.

The supercell storm is a quasi-steady state type of convection that may persist for several hours while moving usually to the right of the mean low level wind. These storms occur with stronger wind shear with the shear vector veering with height for right moving supercells. On rare occasions a wind shear vector backing with height may produce a supercell moving to the left of the mean wind. The usual right moving supercell is associated with a mid level mesoscale cyclonic circulation that gradually propogates downward to the ground. Strong long lived tornadoes, large hail, and high winds are common with this storm type. The wind shear allows the storm to move along its own outflow boundary

so that a continuous supply of warm moist air may feed the storm. The principal updraft occurs near the center of the mesocyclone between the forward and rear flank downdrafts. Sometimes the rear flank downdraft becomes sufficiently strong, so that it wraps around the mesocyclone occluding with the forward downdraft, in an analogous manner to the occlusion of a cold front with a warm front in a synoptic scale low pressure system. If this happens, the storm becomes cut off from its energy source, and sometimes a new supercell develops at the point of occlusion.

Recent numerical cloud modelling experiments of Weisman and Klemp (1982,1984,1986), hereafter referred to as W&K, have produced some remarkable simulations of these three types of convective storms. In their experiments they start the model with a horizontally homogeneous atmosphere with a specified buoyant energy, and give the model a small warm temperature perturbation to initiate convection. The effect of wind shear is examined by keeping all conditions the same and varying the shear. It is shown that given the same degree of instability, the resulting convection ranges from the short lived single cell to supercell storms depending on the prescribed wind shear.

W&K also show that in a weakly unstable atmosphere convection can grow with small wind shear, but dies out in higher wind shear. Likewise, isolated supercell growth occurs in highly unstable conditions with strong wind shear, while weaker convective cells diminish. Instability and wind shear both have an important effect in determining the type of convection that may develop, and they can be combined into a single parameter called the Bulk Richardson Number (BRN) which is the ratio of buoyant energy "B" (positive area on a thermodynamic diagram) to wind shear:

$$BRN = B / .5U^2$$

where U is evaluated by taking the magnitude of the vector difference between the density weighted mean wind over the lowest six kilometers of the wind profile and the mean wind in the lowest 500 meters of the atmosphere.

Model results indicate that supercells develop with BRN less than 50 and multicell storms predominate with BRN greater than about 35. A small sample of observed storms are compared by W&K to the model results and compare very well as shown in Fig. 1.

Another observational study by Rasmussen and Wilhelmson (1983) indicates that tornadic storms may be discriminated from non-tornadic storms by a consideration of potential buoyant energy and a measure of wind shear. Their potential buoyant energy is calculated in a similar manner to the buoyancy "B" of the previous study and represents the positive energy available between the level of free convection (LFC) and the equilibrium level (EL). Their measure of wind shear is different than the shear of W&K. The shear used here is measured from the surface to four kilometers and is the sum of weighted shear vector magnitudes for each 200 meter layer divided by the total depth of 4000 meters.

This method quantifies the shear better in soundings which have large fluctuations in speed and direction seen in looping hodographs. A vector difference between high and low levels tends to underestimate shear with this type of profile.

Their results are shown in Fig. 2, which is a plot of storms primarily from the southern Great Plains region, as a function of shear and buoyant energy. Tornadic storms in this sample fall exclusively in the region of high shear and high potential buoyant energy with non-tornadic storms almost exclusively in the region and lower shear and lower buoyant energy. Stability and shear are computed from the 1200 GMT raob data closest to the storm location with storms generally occurring in the afternoon. Only those cases are shown where there was no significant change of airmass during the period between 1200 GMT and the time of storm occurrence. All cases in which soundings changed due advection or vertical motion during the day were discarded.

Both studies discussed above indicate a potential for using a combination of wind shear and stability from the 1200 GMT raob data to predict the type of convection, if any, that may occur during the afternoon. Since supercell storms are more likely to be associated with severe weather than the single cell or multicell storms, it is possible that these two parameters may be useful for assessing the potential for severe weather in general. Measures of wind shear and stability very similar to those used in the previously mentioned studies are available from an AFOS applications program CONVECT (Stone, 1988) and will be statistically evaluated for their usefulness in assessing severe weather potential over the eastern United States.

II. METHOD

Various wind shear and stability parameters are computed from the 1200 GMT raob data for the fifteen locations in the eastern United States shown in Fig. 3 during the period between 20 April and 30 September 1987. Severe weather occurrences are available daily in the "Tornado and Severe Thunderstorm Reports - Preliminary List" compiled by the National Severe Storms Forecast Center (NSSFC) and distributed via the AFOS product STADTS. Since this is the preliminary list, it may contain a few erroneous reports and some storm reports are usually missing due to their late arrival at NSSFC. Despite its deficiencies, it gives a fairly good indication of severe weather activity and it is readily available. The type of convection, single cell, multicell or supercell that produced the severe weather events is not available in STADTS, and can usually only be obtained by a detailed examination of the radar imagery, which is beyond the scope of this study.

Occurrences of severe weather events between 1800 GMT and 2400 GMT within a 125 nautical mile radius of each raob station in Fig. 3, were compiled. Severe weather is reported in four categories: tornado, large hail greater than 3/4 inch, wind gusts

in excess of 50 knots, and wind damage. Any one of the four types of events was considered a severe weather occurrence in the statistical analysis. Although multiple events frequently occur in the vicinity of the raob station, the only thing considered in the analysis is whether or not severe weather occurred; one event is not considered any differently than a dozen events.

To assess the relationship between the various wind shear and stability parameters and the occurrence or non-occurrence of severe weather in the vicinity, point biserial correlation coefficients are computed for each parameter and multiple correlation coefficients for the entire group of parameters. The point biserial correlation coefficient measures the relationship between a continuous variable, e.g. buoyant energy, and a binary variable, e.g. occurrence or non-occurrence of severe weather events.

III. PARAMETERS AVAILABLE FROM THE 'CONVECT' PROGRAM

1. EI Energy Index

This stability index (Stone, 1984) is a measure of buoyant energy of a parcel. It is computed by selecting the parcel in the lowest 150 mbs of the atmosphere that has the highest wet bulb potential temperature and raising that parcel to the 400 mb level, while entraining environmental air at a rate that provides a 60 percent increase in mass over a 500 mb ascent. The energy index is the sum of positive and negative energy areas as the parcel ascends to the 400 mb level.

2. EI+ Positive part of EI.

3. EI- Negative part of EI.

4. B+ Positive buoyant energy

The same parcel used in EI is lifted to the equilibrium level (EL) and energy areas are computed without entrainment. The positive part is B+ and the negative part B-.

5. B- Negative buoyant energy

6. BRN Bulk Richardson Number

The ratio of positive buoyant energy to the measure of wind shear SHR described below. BRN = B+/SHR.

7. SHR Density weighted wind shear. SHR = $U^2/2$.

U is calculated as the magnitude of the density weighted mean wind vector from the surface to 6 kilometers minus the mean wind of the lowest 500 meters. Used by Weisman and Klemp (1986).

8. SS5 Speed shear to 5 thousand feet above ground level (AGL).

Computed by summing the magnitude of wind shear vectors in thousand foot increments from the surface to 5 thousand feet AGL according to the formula:

$$SS(N) = \frac{1}{N} \sum_{i=1}^{N} |\underline{V}_i - \underline{V}_{i-1}|$$

where N = 5.

9. SS10 Speed shear to 10 thousand feet AGL
Computed as above with N = 10.

10. SS15 Speed shear to 15 thousand feet AGL
Computed as above with N = 15. This measure of shear is approximately the same as that used by Rasmussen and Wilhelmson (1983).

11. VS5 Vector product shear to 5 thousand feet AGL
See 13 below.

12. VS10 Vector product shear to 10 thousand feet AGL
See 13 below.

13. VS15 Vector product shear to 15 thousand feet AGL
The vector product shear is a measure of wind shear that combines both the variation of wind direction and wind speed with height. It is computed in three steps:

i. Wind vectors are interpolated from standard reporting levels to one thousand foot increments from the surface to 16 thousand feet AGL.

ii. The resulting wind hodograph is smoothed by averaging the wind at each level with the level above and below it, according to the formula:

$$\underline{V}_i = \frac{1}{3} (\underline{V}_{i-1} + \underline{V}_i + \underline{V}_{i+1})$$

where i = 0...15, and $\underline{V}_{-1} = \underline{0}$.

iii. The vector product shear is defined as the sum of the signed magnitudes of vector products of the smoothed shear vectors in thousand foot increments according to the formula:

$$VS(N) = \sum_{i=1}^{N} \underline{k} \cdot (\underline{V}_i - \underline{V}_{i-1}) \times (\underline{V}_{i-1} - \underline{V}_{i-2})$$

where N = 5, 10, 15 for VS5, VS10, and VS15, respectively, $\underline{V}_{-1} = \underline{0}$, and $\underline{k}$ is the positive unit vector in the vertical.

The vector product shear is illustrated schematically with the smoothed wind hodograph shown in Fig. 4. Since the magnitude of a vector product is equal to the area of a parallelogram that lies between the two vectors, the vector product shear as defined above is the sum of the areas of the parallelograms delineated by the hodograph. The vector product shear is positive, if the shear vectors veer with height and negative, if they back with height. If there is no variation of the wind shear direction with height,

then the contribution to the vector product shear is zero, even though significant speed shear may exist.

In the illustration of Fig. 4 the shear vector veers with height to three thousand feet and the contribution to VS5 is the positive sum of areas of the first three parallelograms; above three thousand feet the shear vector backs with height and the final two parallelograms make a negative contribution to VS5, but their sum is not large enough to cancel the large positive sum below three thousand feet, so VS5 is positive in this example.

IV. RESULTS

Point biserial correlation coefficients between the various stability and wind shear parameters and occurrence of severe weather are shown in the first thirteen lines of Table 1. The first column of the table showns coefficients obtained from the complete data sample consisting of 1755 cases, approximately 73 percent of the potentially available data for this period. Only operationally available data were used in this study. Some data were lost due to communications failure or computer failure that prevented the data collection program from operating. No attempt was made to retrieve data missing for any reason. Cases were excluded from the sample, if any portion of the data was missing, e.g. winds not available to 16 thousand feet, EI missing, etc. The only exception occurs with the parameters B+ and B-, which are not defined unless the EL is at some distance above the ground. On very stable days EL is on the ground, there is no positive area, so B+ and B- are not available. This is the reason correlation coefficients are not computed for B+, B-, and BRN in the first column of Table 1. All other parameters can be computed, if the raob is complete.

Table 1 shows that when the full data sample is considered, the best correlation to severe weather is obtained from EI+ with a coefficient of .288. This is somewhat better than the correlation of EI (the sum of EI+ and EI-) at .256. A multiple correlation of all parameters using a screening regression process shows that a combination of EI+ and EI- yield a correlation of .300 (line 14).

The correlation of all wind shear measures is very poor with the best being SHR at -.067. The screening regression program picked the vector product shear VS15 as the third best predictor, but when combined with EI+ and EI- the multiple correlation is only increased to .303, an insignificant improvement over .300 for the EI+ and EI- combination. Although wind shear organizes convection and may be useful in determining its type and intensity, we will show that it can be used as a general predictor of severe weather only under special circumstances.

Previous studies have demonstrated that EI is well related to general thunderstorm activity (Hicks et.al., 1986) and when the morning EI is positive it has been shown that the probability of afternoon thunderstorms in the vicinity is 90 percent or more

(Stone, 1985,1986). Therefore, we extract a subset of the data, in which EI is positive and the EL is above ground level so that B+, B-, and BRN are available and we are confident that at least 90 percent of this sample consists of thunderstorm days. The correlations of the various parameters of this subset, consisting of 506 cases, is shown in column 2 of Table 1.

The best correlation to severe weather is still EI+ but the coefficient has now dropped to .145. Note that the correlation of EI- has become negative. This means that favorable conditions for severe weather exist when a large EI+ is associated with a large negative EI-. This is evidence of the lid phenomenon (Carlson, 1982), in which the negative energy area near the bottom of the raob sounding suppresses convection until sufficient heating takes place to let parcels break through the lid and utilize the large positive area aloft to produce severe convection. When EI+ and EI- are combined for multiple correlation, the result is a coefficient of .180. The buoyant energies B+ and B= have a similar relationship to severe weather and when we combine them the multiple correlation is .185, not a significant improvement over the EI+, EI- combination.

The more important thing about this relatively unstable set of data with positive EI, is that wind shear, in particular the vector product shear, is now more closely related to severe weather occurrence. The shears SHR, SS5, SS10, and SS15 are now positively correlated to severe weather, but the coefficients remain small. This indicates that severe weather is weakly related to strong speed shears on days with high buoyant energy. The more significant increase in correlation is seen in the vector product shears, with VS15 being best with correlation .142, almost as good as EI+ with .145. The screening regression programs selects VS15 as the best wind shear predictor and yields a multiple correlation of .229 when combined with EI+ and EI-.

The bulk Richardson Number, BRN, gives rather disappointing results with a correlation of only .053. The cloud modelling studies of Weisman and Klemp (1982,1984,1986) indicate that BRN is well related to the type of convection, single cell, multicell, or supercell and this is also supported by a limited sample of observational data. The poor correlation of BRN may be due to the fact that supercell convection is more uncommon in the East, and the majority of our sample of severe weather events is probably due to multicell storms. However, it is also possible that the wind shear, SHR, used in computing BRN is not sufficiently well related to supercell convection. Although supercells can be generated in the Klemp-Wilhelmson cloud model using a straight line hodograph, in nature, the supercell almost always occurs with the shear vector veering with height, which provides a supercell moving to the right of the mean wind. It seems likely that a measure of wind shear such as the vector product shear, which accounts for the rotation of the shear vector with height, may be better related to supercell convection. Nevertheless, the vector

product shear is clearly the better predictor of severe weather than any of the speed shears.

Our sample of thunderstorm days with positive EI is then split into two parts, one for the spring season, April through June, and summer, July through September. The results are shown in columns 3 and 4 of Table 1. This split reveals a very significant result, namely, that wind shear is highly correlated with severe weather in the spring and virtually uncorrelated in the summer.

During the spring season (column 3) the vector product shear VS15 shows the best correlation with a coefficient of .301, slightly better than VS5 and VS10; second best are the speed shears SS5, SS10, SS15 followed by SHR. It is interesting that the correlation of vector product shear is about the same whether it is computed to 5, 10, or 15 thousand feet. This indicates the the most important part of the shear is in the first five thousand feet, although, a small increase in correlation is achieved by computing to 15 thousand feet.

It is interesting that stability (buoyant energy) is not well correlated during the spring season. Even the multiple correlation coefficient of EI+ and EI- is only .139 and the B+, B- combination is .121. The screening regression yielded the best correlation .334 with the combination of EI+, EI-, and VS15; the fourth parameter selected was SS15, but this increased the correlation only to .336, an insignificant improvement.

When we examine the correlations from the summer season, July through September, the importance of buoyancy and wind shear are reversed. In this case, the best stability measure is EI+ with a correlation of .179 and when combined with EI- this rises to .210, while the B+, B- combination is slightly better at .222. All the wind shears are very poorly correlated to severe weather in the summer and multiple correlation coefficients are not significantly improved when wind shear is combined with buoyancy.

The end result is that the vector product wind shears are well related to the occurrence of severe weather on unstable days during the spring season, but they are almost worthless as a predictor during the summer. Although our study is based on a relatively small sample, we believe the results are essentially correct, since they agree with a subjective evaluation of the same parameters during the 1986 season in which no statistics were kept.

Histograms of relative frequency of severe weather for various ranges of the vector product shear VS15 are shown in Fig.5 for both spring and summer seasons. The histogram for the spring season shows a clear relationship between VS15 and frequency of severe weather; high values of VS15 are more frequently associated with severe weather than low values. In this data sample, VS15 exceeding the value 18 had a 67 percent frequency of severe

weather. Conversely, the histogram for the summer season shows little, if any, relationship between VS15 and frequency of severe weather. Since the range of values of VS15 are similar during spring and summer, it seems likely that the difference between the seasons may be attributed to the varying influence of dynamic forcing. During the spring dynamic forcing is substantially stronger than during the summer months. It appears that favorable wind shear combined with dynamic forcing initiates severe convection in the springtime, but during the summer favorable wind shear is usually not accompanied by sufficient forcing to trigger severe weather. As shown in Table 1 summertime severe weather is more related to the available buoyant energy.

Rasmussen and Wilhelmson (1983), hereafter referred to as R&W, investigated the relationship of afternoon tornadic storms to both potential buoyant energy (PBE) and wind shear computed from the 1200 GMT soundings. A sample of storms primarily from the southern Great Plains was selected which includes tornadic storms, non-tornadic storms with mesocyclones, and storms without mesocyclones. The sample was carefully selected, discarding cases where the sounding was affected by nighttime or early morning convection, and eliminating cases in which the sounding changed significantly during the day due to advection or vertical motion. The storms were plotted on a graph (Fig. 2) with shear and PBE as axes, with all tornadic storms falling in the area of high PBE and high shear, storms without mesocyclones fall in the area of low PBE and low shear, and non-tornadic storms with mesocyclones in between the previous two.

Our sample of severe weather is not carefully selected, but consists of all possible cases that our data collection program was able to record. As mentioned previously we have no record of the type of convection that produced the severe weather, but we do have the severe weather events identified according to type: tornado, large hail, or high wind. Our speed shear SS15, which is computed to 15 thousand feet AGL is almost the same as the R&W shear computed to four kilometers. Likewise, our stability measure B+ is approximately the same as the R&W PBE; both are computed between the level of free convection LFC and the EL. Our sample consists of 153 severe weather cases during both spring and summer seasons, of these, 27 are tornadoes. We would like to distinguish the tornadic from the non-tornadic severe weather in the manner of R&W.

The result is shown in Fig. 6 with 'x' plotted for tornado and 'o' for non-tornadic severe weather as a function of SS15 and B+. Unfortunately, tornadoes and non-tornadic severe weather seem to be randomly interspersed. Similar plots using other measures of shear and buoyancy produced no better results. In our data sample tornadic and non-tornadic storms cannot be distinguished using the shear-buoyancy graph.

There are several possibilities for the difference between our results and those of R&W. First, the geographic area is

different. Supercell storms are not as common in the East as in the southern Great Plains. The tornadoes in our sample are not necessarily from supercell storms, perhaps none of them are; we do not know. The R&W data sample consisted exclusively of supercell tornadoes and the data were carefully screened to remove cases where buoyancy and shear changed drastically during the day. Our data sample is not screened at all and undoubtedly contains cases where buoyancy and shear change completely between the 1200 GMT raob sounding and the occurrence of severe weather in the afternoon. Perhaps a more carefully collected data set would reveal a relationship between shear, buoyancy, and tornadic storms in the eastern United States, but our present data shows none.

V. CONCLUSION

Both buoyant energy and wind shear contribute to creating an atmospheric environment favorable for the development of severe weather. Convection may begin when a sufficient amount of buoyant energy is present in the atmosphere. Three dimensional cloud models and observational evidence indicate that the type of convection that develops is related to the wind shear. Weak wind shear is associated with single cell convection, moderate shear produces multicell storms, and stronger speed shear with a clockwise rotating shear vector in the lowest levels are typical of supercell storms. Severe weather may occur with both multicell and supercell storms, but the stronger severe weather and long-lived tornadoes are most common with the supercell storms.

On unstable days when afternoon thunderstorm activity is likely, we find that wind shear, in particular the vector product shear (VS5, VS10, or VS15), is fairly well related to the occurrence of severe weather. The difference we obtain between the spring (April-June) and the summer (July-September) seasons is quite significant. The vector product shear has a good relationship to severe weather in the spring, but very little relationship in the summer. Since similar shears occur in both seasons, it seems likely that the stronger dynamic forcing that occurs in the spring supports the wind shear resulting in supercell type storms, while during the summer the general lack of dynamic forcing precludes supercell development.

Supercell storms are not as common in the East as in the Midwest. Some storms develop in the east that have supercell characteristics but lack the intensity of the Midwest type supercell. This type of eastern storm does not always produce tornadoes, but frequently produces high winds and large hail. The significant correlation we obtain between shear and springtime severe weather is probably the result of this type of storm. The summertime severe weather seems to be primarily associated with multicell storms and we find little relationship to wind shear. During the summer season airmass type thunderstorms are more common and they typically occur where instability is greatest. However, even during the summer, some weak mesoscale or synoptic scale forcing is usually needed to produce severe weather.

We also find that positive buoyant energy as measured by the parameter EI+ is better correlated with severe weather than the energy index EI, which is the sum of EI+ and EI-. EI-, the negative buoyant energy area, is negatively correlated to severe weather, which seems to be a result of a lid phenomenon, which suppresses convection until the lid is broken by sufficient solar heating which allows severe convection to begin at that point. The EI buoyant energy measure uses a parcel having maximum wet bulb potential temperature in the lowest 150mb of the atmosphere, and energy is computed up to the 400 mb level. The B+ measure of buoyant energy has been used by most investigators and represents the energy between the LFC and EL. We find that correlations to severe weather are similar for both of them, but since EI may always be computed, whereas, B+ may be computed only on unstable days, we prefer the EI energy measure. Both buoyant energy and wind shear computed from the morning raob sounding can be used to assess the potential for severe thunderstorms during the afternoon.

If the atmosphere is sufficiently unstable to support afternoon convection, the type of convection that results depends on the amount of buoyant energy available and the wind shear structure, and the amount of dynamic forcing available, if any. Our study has neglected this third factor, but significant severe weather outbreaks are nearly always associated with some dynamic forcing, either mesoscale or synoptic scale. The degree of instability and the wind shear structure combined determine the atmospheric response to whatever forcing that may be imposed. We have found that a useful predictor for assessing atmospheric response is a linear combination of EI+, EI-, and VS15, but the combination B+, B-, and VS15 yields an equally good predictor.

Although Weisman and Klemp (1984) found that BRN was a good indicator of the type of convection that may occur, our results do not confirm it's value in the eastern United States. We believe that buoyant energy and wind shear are more useful considered seperately and should not be combined into a BRN.

We did not find buoyant energy and wind shear to be useful in distinguishing between tornadic and non-tornadic storms. R&W did find a useful relationship for Midwest storms, so it may be that the scarcity of supercell tornadoes in the East is the problem.

Finally, we should recall that all our results are based on buoyant energy and wind shear computed from the 1200 GMT raob data and correlations are then made with afternoon severe weather. Conditions can change significantly over this six to twelve hour period, the atmosphere can stabilize or destabilize, and shear can become more or less favorable as the day progresses. The NEXRAD Doppler radars that will be deployed in the early 1990's will have the capability of monitoring the low level wind profile at frequent time intervals. There is also a possibility that a wind profiler network may be established in the future. With the

advent of this new technology we will be able to observe the change in the wind hodograph periodically through the day and thus assess the progression to a favorable or unfavorable shear condition for severe convection. Meanwhile, the wind shear, especially in the springtime, should still be an important consideration in determining the potential for afternoon severe weather.

A case study of an early season severe weather outbreak in eastern Ohio and western Pennsylvania is given in the appendix. It illustrates the importance of wind shear, interacting with instability and dynamic forcing, in creating a favorable environment for the development of severe weather.

VI. REFERENCES

Carlson, T.N., 1982: The Role of the Lid in Severe Storm Formation: Some Synoptic Examples from SESAME, Preprints, 12th Conf. on Severe Local Storms, San Antonio, Texas, Amer. Meteor. Soc., 221-224.

Hicks, T.M., J.D. Schumacher, and G.K. Grice, 1986: An Evaluation of Seven Stability Indices as Predictors of Convection in South Texas, NOAA Technical Memorandum, NWS SR-119, National Weather Service, San Antonio, Texas.

Rasmussen, E.N. and R.B. Wilhelmson, 1983: Relationships Between Storm Characteristics and 1200 GMT Hodographs, Low-level Shear and Stability, Preprints, 13th Conf. on Severe Local Storms, Tulsa, OK, Amer. Meteor. Soc., J5-J8.

Stone, H.M., 1984: The Energy Index for Stability, Preprints, 10th Conf. Wea. Forecasting and Analysis, Clearwater Beach, Fla., Amer. Meteor. Soc., 550-554.

Stone, H.M., 1985: A Comparison Among Various Thermodynamic Parameters for the Prediction of Convective Activity - Part II, NOAA Technical Memorandum, NWS ER-69, National Weather Service, Garden City, NY.

Stone, H.M., 1986: A Comparison Among Various Thermodynamic Predictors of Convection, Preprints, 11th Conf. Weather Forecasting and Analysis, Kansas City, Mo., Amer. Meteor. Soc., 241-246.

Stone, H.M., 1988: Convective Parameters & Hodograph Program - CONVECT, NOAA Eastern Region Computer Programs and Problems, NWS ERCP-37 Revised, National Weather Service, Garden City, NY.

Weisman, M.L. and J.B. Klemp, 1982: The Dependence of Numerically Simulated Convective Storms on Vertical Wind Shear and Buoyancy, Mon. Wea. Rev., 110, 504-520.

Weisman, M.L. and J.B. Klemp, 1984: The Structure and Classification of Numerically Simulated Convective Storms in Directionally Varying Wind Shears, Mon. Wea. Rev., 112, 2479-2498.

Weisman, M.L. and J.B. Klemp, 1986: Characteristics of Isolated Convective Storms, Mesoscale Meteorology and Forecasting, Ed. P.S. Ray, Amer. Meteor. Soc., 331-358.

APPENDIX

The first severe weather of 1987 in the Eastern Region occurred during the afternoon and evening of March 25th, about a month before we began gathering data for the statistical study of this report. Large hail up to 1.75 inches in diameter was observed over portions of West Virginia, eastern Ohio, and western Pennsylvania. The preliminary severe weather list (STADTS) from NSSFC and the corresponding plot are shown in Fig. 7. This weather occurred in advance of a cold front that moved into western Pennsylvania later in the evening.

The 850mb chart for 1200 GMT is shown in Fig. 8. The low center is in extreme northwest Missouri with cold air advecting around the south side of the low and the ridge is along the east coast. The 500mb chart (Fig. 9) shows that the circulation is nearly vertically stacked. The main positive vorticity advection is in Michigan and southern Ontario. A minor vorticity lobe in western Tennessee is advecting toward the northeast and provides some weak dynamic forcing for the severe weather that occurs later in the day.

The energy index EI, shown in Fig. 10, indicates the principle buoyant energy in the Carolinas and Georgia with a relatively unstable tongue extending toward the north into Ohio. The vector product shear VS15 is shown in Fig. 11. The largest values, where convection is favorable, lies through the area of West Virgina, eastern Ohio, and western Pennsylvania, approximately the same area where the severe weather occurred. The hodograph for Pittsburgh (Fig. 12) shows the characteristic veering of the shear vector with height and strong speed shear, particularly in the levels below five thousand feet. It is readily seen that the principle contribution to the VS15 shear comes from these lower levels; the hodograph is nearly a straight line between seven thousand and sixteen thousand feet MSL.

The main point is that severe weather occurred where wind shear is favorable, in a weakly unstable area, with some dynamic forcing due to the approaching front and weak positive vorticity advection that develops later in the day. All three factors, shear, instability, and dynamic forcing, come together during the afternoon to produce this outbreak of severe weather. The severe weather did not occur further south in the Carolinas where instability was greater, because shear conditions were not quite as favorable and dynamic forcing was absent.

Table 1

Point biserial correlation coefficients between various parameters from the 1200 GMT raobs and severe weather observed during the period 1800-2400 GMT.

		1	2	3	4
		All EI APR-SEP	EI > 0 APR-SEP	EI > 0 APR-JUN	EI > 0 JUL-SEP
No. Cases		1755	506	186	320
1	EI	.256	.122	.069	.154
2	EI+	.288	.145	.091	.179
3	EI-	.221	-.067	-.078	-.062
4	B+		.123	.078	.153
5	B-		-.136	-.092	-.159
6	BRN		.053	-.072	.138
7	SHR	-.067	.031	.120	-.010
8	SS5	-.022	.066	.205	-.012
9	SS10	-.064	.058	.207	-.017
10	SS15	-.062	.068	.210	.001
11	VS5	.051	.119	.291	.018
12	VS10	.049	.138	.292	.049
13	VS15	.048	.142	.301	.049
Multiple correlation coefficients:					
14	EI+,EI-	.300	.180	.139	.210
15	EI+,EI-,VS15	.303	.229	.334	.215
16	B+,B-		.185	.121	.222
17	B+,B-,SHR		.196	.179	.227
18	B+,B-,VS15		.240	.328	.232

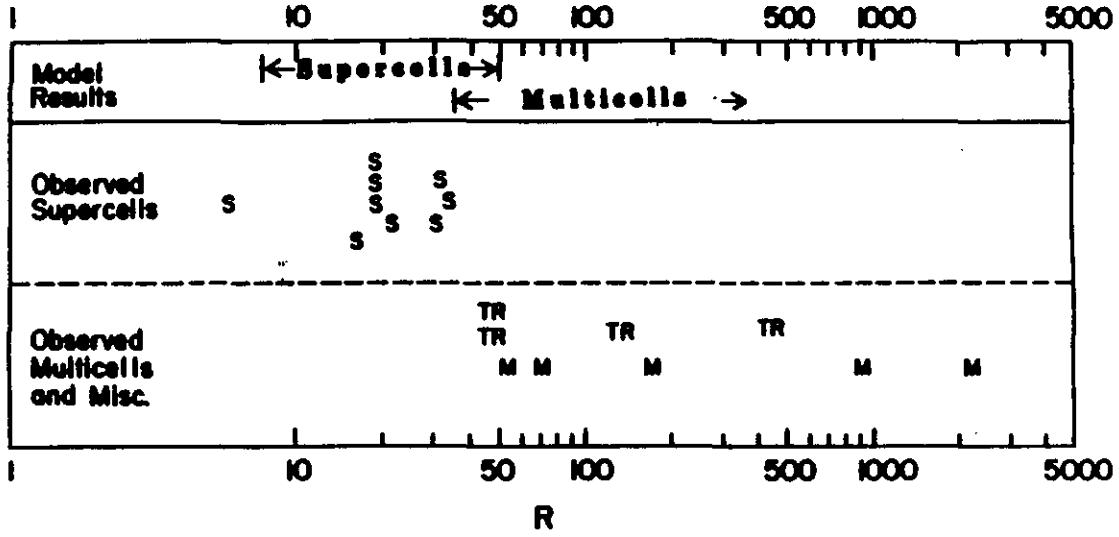

Fig. 1. Relationship of Bulk Richardson number to various storm types. 'S' denotes supercell and 'M' multicell storms. 'TR' denotes storms in a tropical atmosphere. Observed 'S' and 'M' storms shown are from Midwest area. (adapted from Weisman and Klemp, 1986).

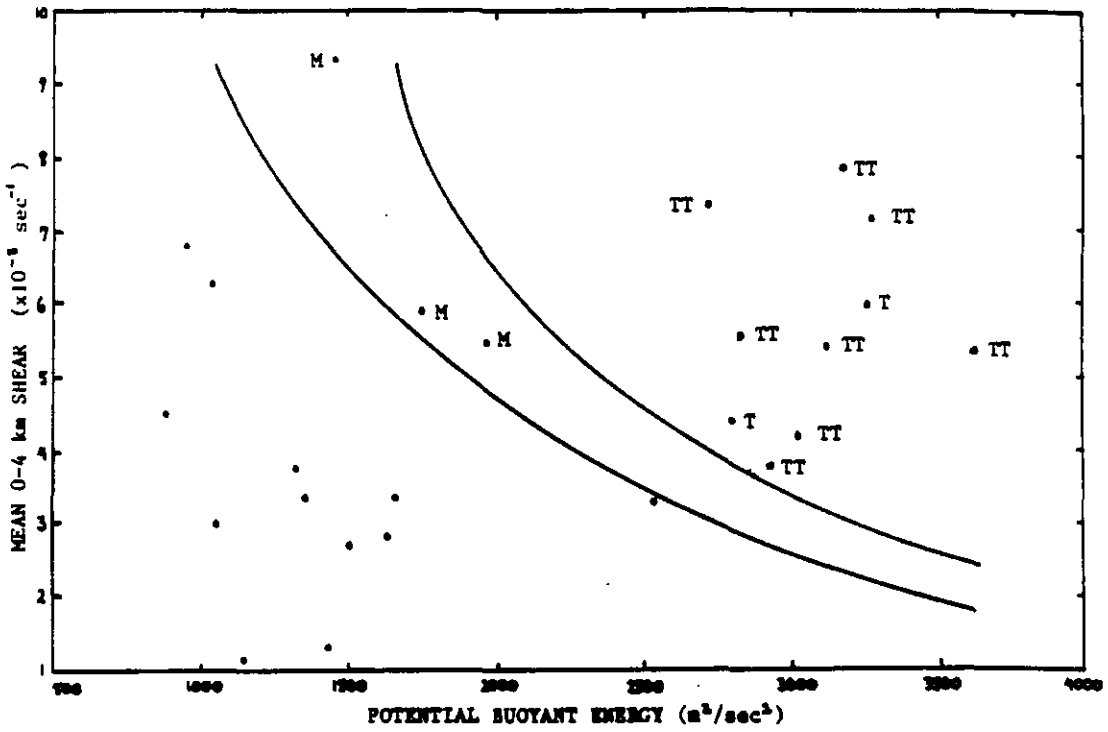

Fig. 2. Storm type as function of 0-4 km mean shear and potential buoyant energy. 'T' denotes storm with one tornado, 'TT' storm with multiple tornadoes, 'M' storm with mesocyclone, and a single point a storm without mesocyclone or tornado. (adapted from Rasmussen and Wilhelmson, 1983).

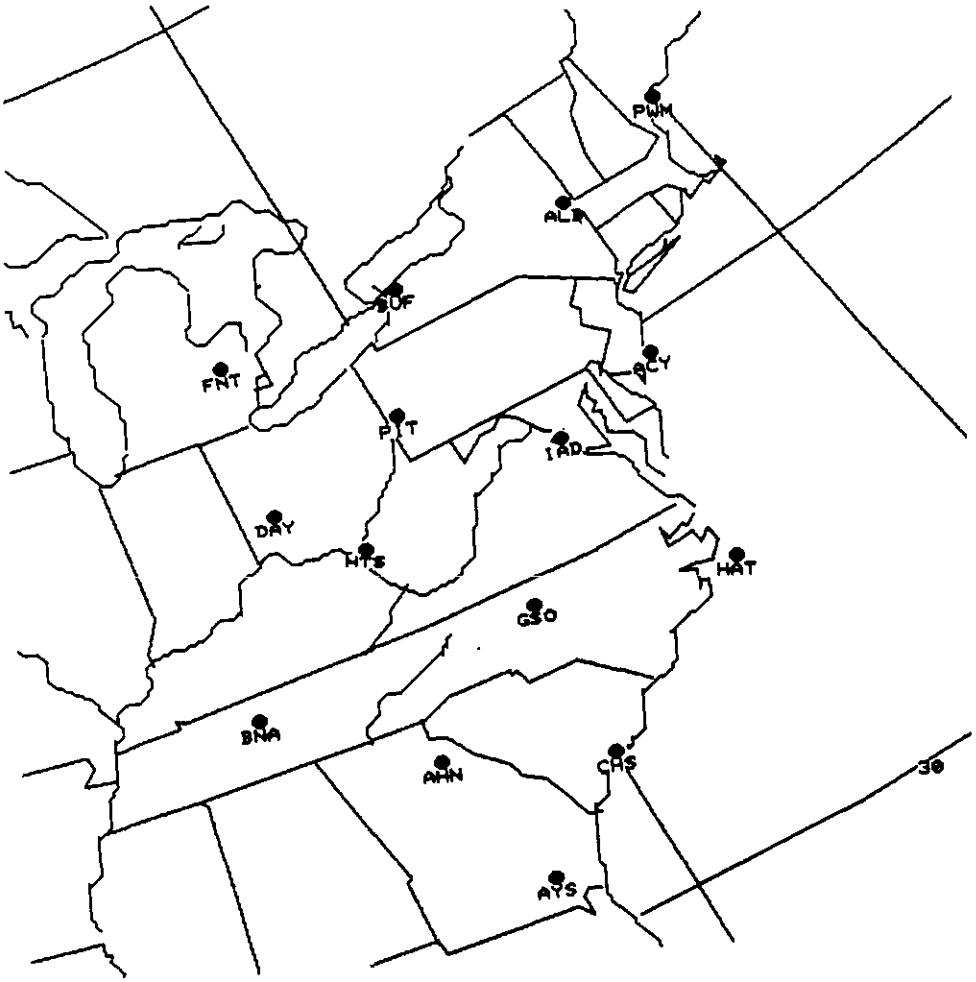

Fig. 3. Stations at which stability and wind shear are computed.

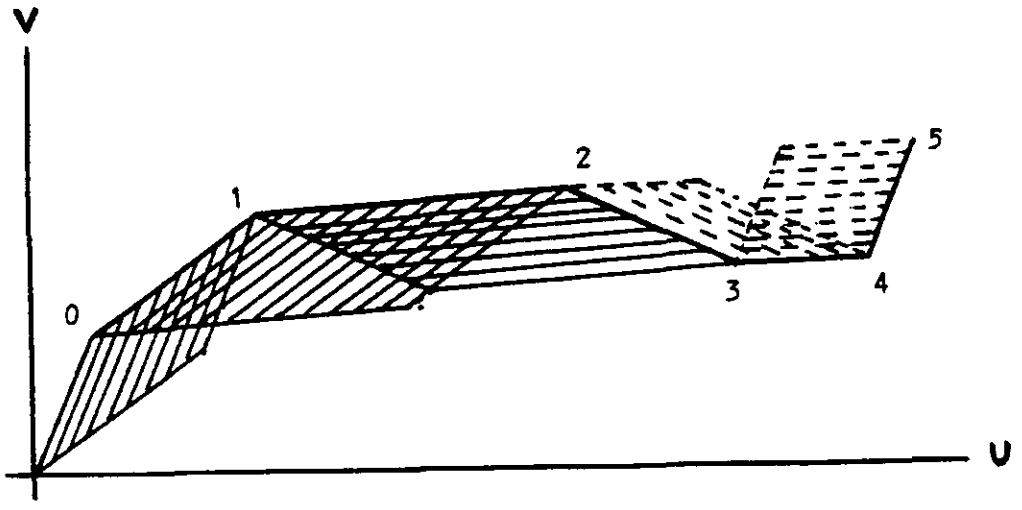

Fig. 4. Smoothed wind hodograph from the surface '0' to five '5' thousand feet AGL, illustrating the computation of the vector product shear VS5. Solid shaded parallelograms indicate positive areas where the shear vector is veering with height and dashed shaded parallelograms are negative areas where shear vector is backing with height. The shear VS5 is the sum of the areas.

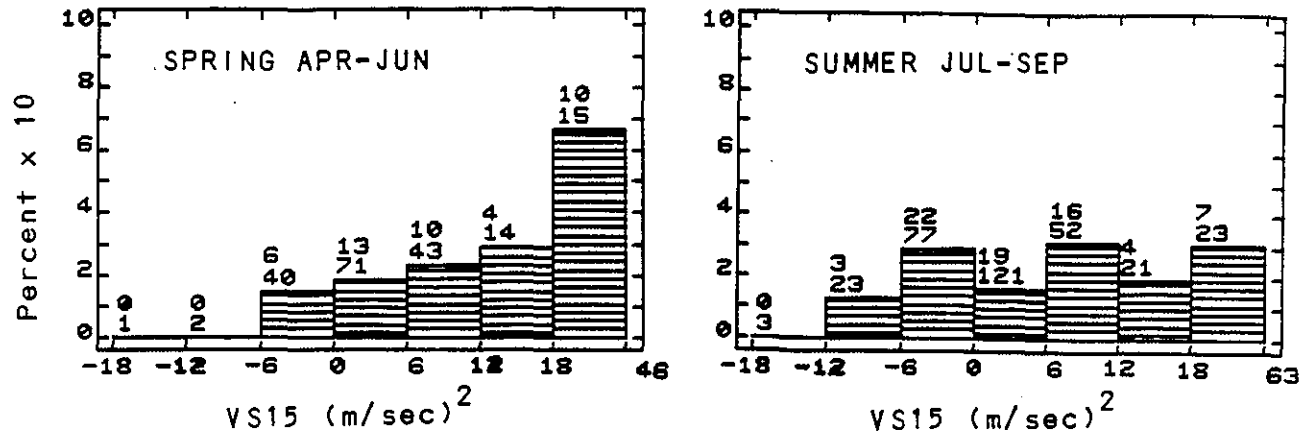

Fig. 5. Histograms of relative frequence of occurrence of afternoon severe weather (1800-2400 GMT) versus vector product shear, VS15, computed from morning raobs (1200 GMT) for spring and summer seasons. Top number above each bar is number of severe weather occurences and bottom number is total number of cases in that interval. The extreme right bar in both graphs represents all cases with VS15 greater than 18. Observed range of VS15 in spring is -17 to 46, and summer -17 to 63.

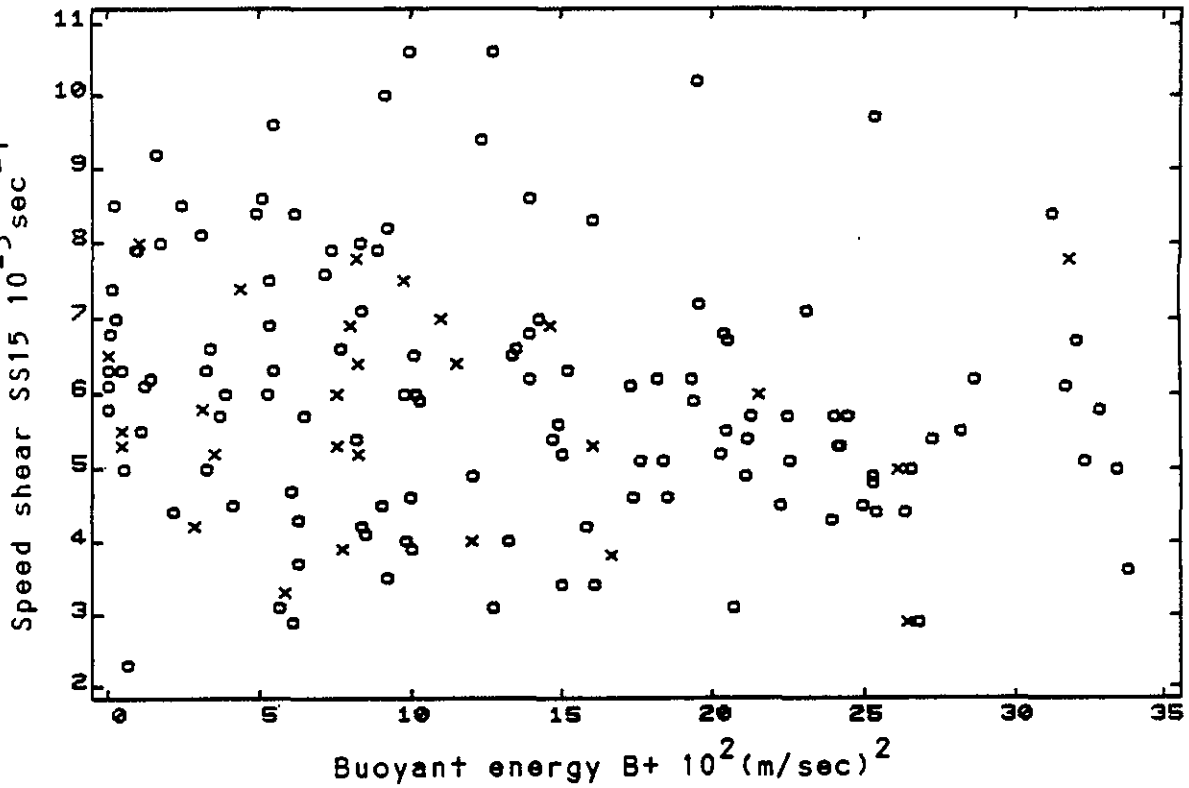

Fig. 6. Scatter diagram of tornadic 'x' and non-tornadic 'o' severe storms as a function of speed shear to 15 thousand feet, SS15, and buoyant energy, B+. Sample consists of 153 severe weather events including 27 tornadoes, over the period Apr.20 to Sep.30.

MKCSTADTS
WOUS80 KMKC 260933

NSSFC TORNADO and SEVERE THUNDERSTORM REPORTS
Preliminary List - Internal Dissemination Only
for 06CST WED MAR 25 1987 thru 06CST THU MAR 26 1987

	Event	Location	Remarks	(CST) Time
1	A125	NR ZELIENOPLE PA	(21 NNE PIT)	(-----) 25/1305
				PIT/SVR 4000 8013
2	A 75	HARPERSFIELD OH	(38 NNW YNG)	(-----) 25/1638
		DIME SIZE HAIL		CLE/SVR 4176 8095
3	A175	MILTONSBURG OH	(36 NNE PKB)	(-----) 25/1710
		GOLFBALL SIZE HAIL		CAK/SVR 3903 8116
4	A175	GLENDALE WV	(16 SSW HLG)	(-----) 25/1710
		GOLFBALL SIZE HAIL		PIT/SPS 3994 8075
5	A175	WHEELING WV	(8 SSW HLG)	(-----) 25/1725
		GOLFBALL SIZE HAIL		PIT/SPS 4006 8071
6	A100	WEST ALEXANDER PA	(9 ESE HLG)	(-----) 25/1730
				PIT/SPS 4011 8050
7	A 75	WHEELING WV	(8 SSW HLG)	(-----) 25/1750
				PIT/SPS 4006 8071

PAGE 01

Fig. 7. Severe weather listing (STADTS) and plot for the 24 hour period ending 12Z 3/26/87. Large hail is denoted by 'A'.

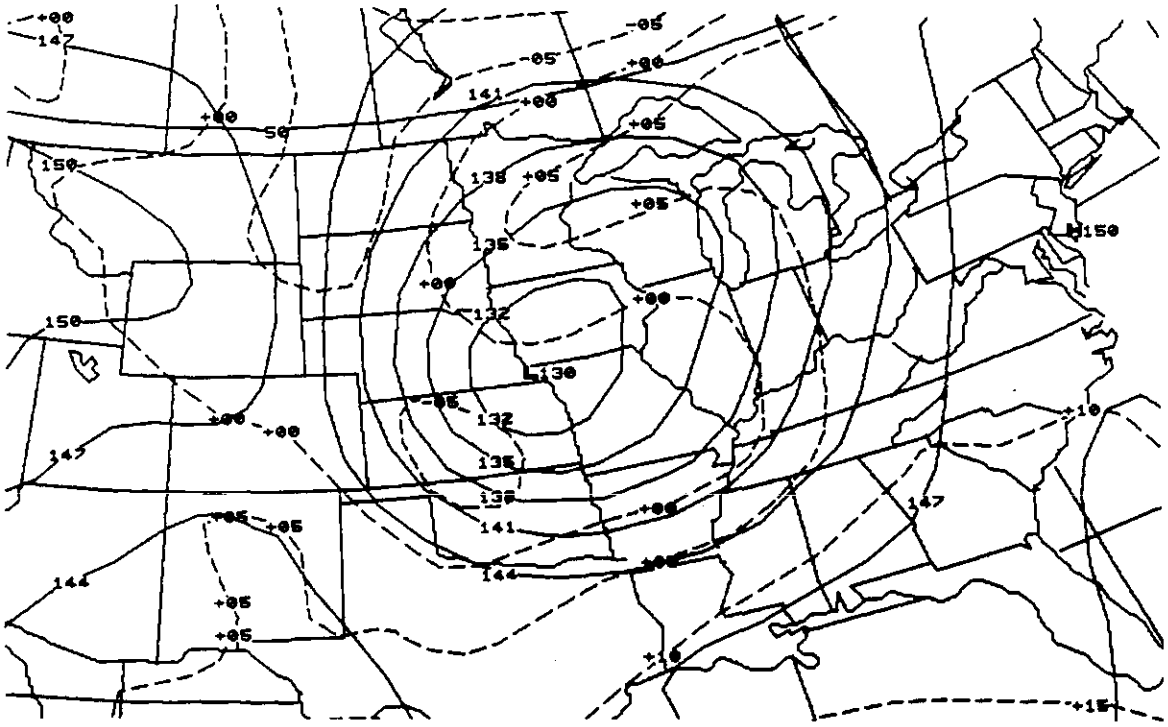

Fig. 8. 850mb height and temperature for 12Z 3/25/87.

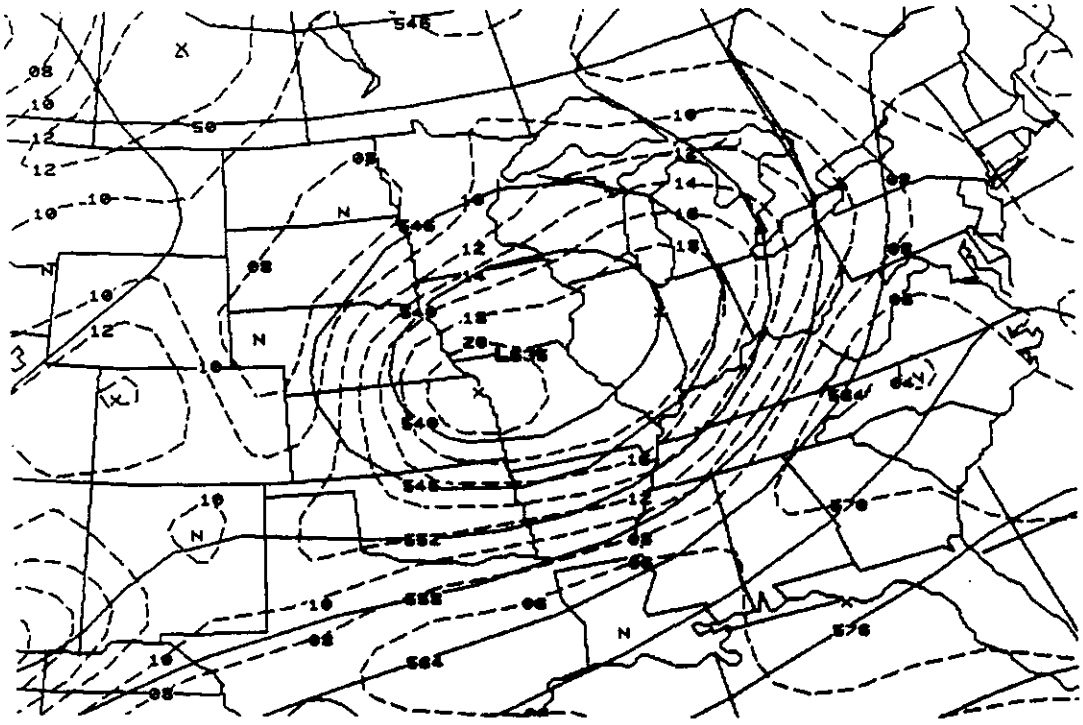

Fig. 9. 500mb height and vorticity for 12Z 3/25/87.

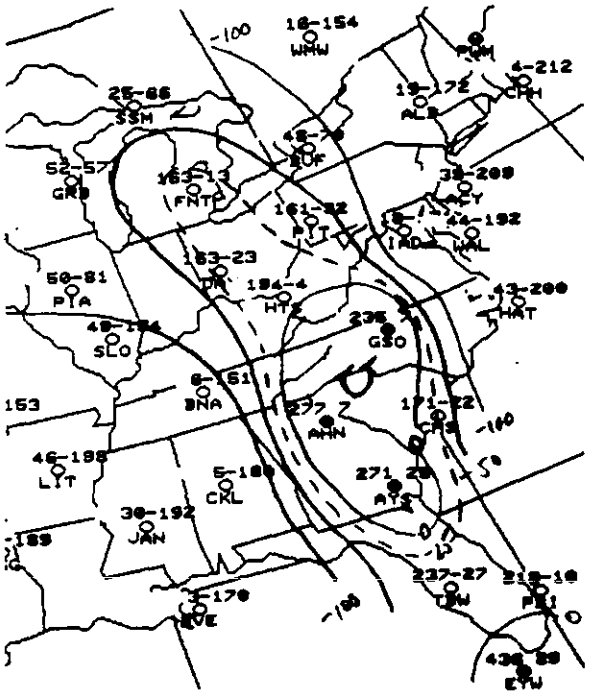

Fig.10. Energy index for 12Z 3/25/87. EI plotted at upper right of station circles. Units: J/Kg x 10.

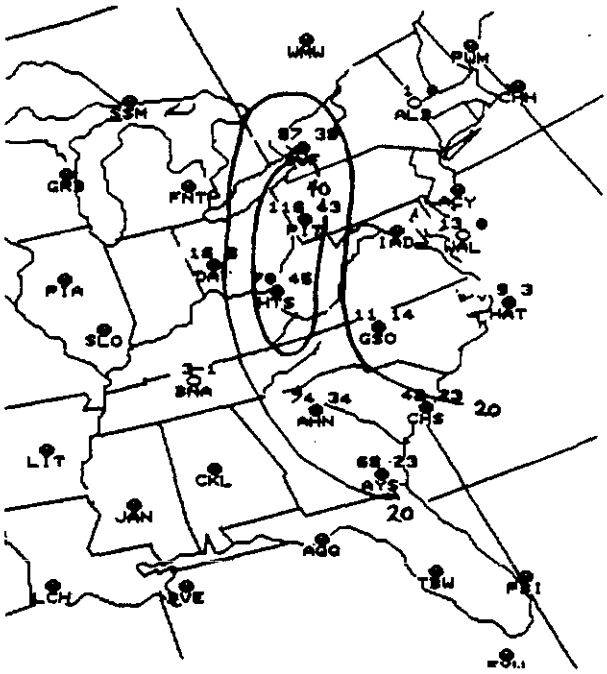

Fig.11. VS15 for 12Z 3/25/87. VS15 plotted at upper right of station circles. Units: $(m/sec)^2$

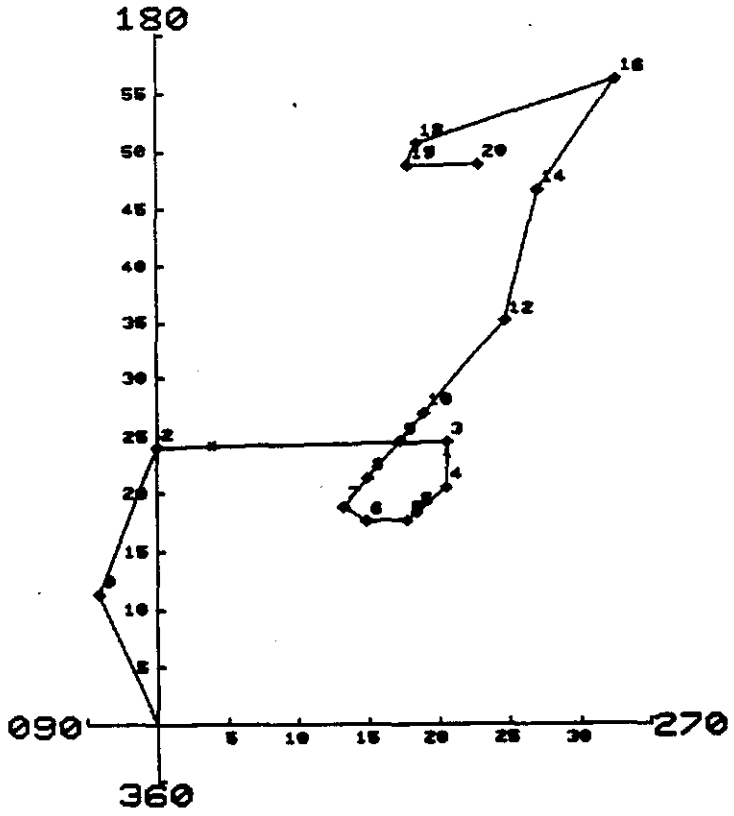

Fig.12. Pittsburgh hodograph at 12Z 3/25/87. Units are knots at standard reporting levels labelled in thousands of feet MSL. Zero '0' indicates surface wind.